# A New Driving Method for Synchronous Rectifiers of LLC Resonant Converter with Zero-Crossing Noise Filter


Dong Wang *Member, IEEE* dong.wang@queensu.ca
Liang Jia *Student Member, IEEE* liang.jia@queensu.ca
Jizhen Fu *Student Member, IEEE* jizhen.fu@queensu.ca
Yan-Fei Liu *Senior Member, IEEE* yanfei.liu@queensu.ca
Paresh C Sen *Life Fellow, IEEE* senp@queensu.ca
Department of Electrical and Computer Engineering, Queen's University
Kingston, Ontario, Canada. K7L 3N6



***Abstract* -- A new driving method for SR is presented. By applying a zero-crossing noise filter to the MOSFET, the false-triggering of the SR can be effectively eliminated. Moreover, the resistor and the capacitor in the filter can be used as a compensator to solve the duty cycle loss issue caused by the trace inductance of the MOSFET package. Only three passive components are needed in the proposed filter which makes it reliable and easy to implement. Simulation and experimental results show that the zero-crossing noise filter can significantly improve the reliability as well as the efficiency of the power circuit. A prototype of 400V to 12V 600W half bridge LLC resonant converter is built to verify the advantages of the new zero crossing noise filter.**



***Index Terms*-- Driving signal, Resonant converter, Synchronous rectifier**


## I. INTRODUCTION

With the development of the computer technology, the demand for the converters with low voltage and high output current keeps increasing. Because of its advantages, the LLC resonant converter with synchronous rectifier (SR) becomes one of the promising solutions[1]. To achieve the high efficiency, the parameter designing of the LLC resonant tank should be optimized[2]. In addition, the driving signal of the SR should be precisely synchronized with the current through the rectifier[3].

Due to the phase shift introduced by the resonant components, the secondary side currents of the LLC resonant converter are not exactly in phase with the switching actions of the primary side MOSFETs[3, 4]. To generate accurate driving signal for the secondary side SR, many studies and efforts have been done in the recent years[1, 3-7]. All of these schemes can be divided into current based method[5-7] and voltage based method[1, 3, 4].

Current based method detects the current through the SR to generate the gate drive signal[5, 8]. The main problems of these methods are the large size of the current-sensing transformer (CT), the extra conduction loss of the winding and the undesired delay that will cause duty cycle loss of the SR and therefore more conduction loss[4, 5, 7]. To avoid the problems mentioned above, primary current sensing with magnetizing current cancellation method is proposed in [5] and [7]. The efficiency of the circuit can be improved because of the relatively smaller primary current of the transformer through the CT. However, the CT and the matching circuits of the transformer magnetizing current make the implementation complex. The matching of the magnetizing current with the inductor or the transformer is also difficult.

Voltage based method detects the voltage across the drain to the source ($v_{DS}$) of the SR to generate the driving signal. Special driving chips have been developed based on this method to simplify the SR driving. However, due to the small $R_{ds\_on}$ of the MOSFET, the voltage rating of the detecting threshold is only at the millivolt level. Thus even a very small zero-crossed ringing caused by the parasitic parameters of the circuit may result in the false gate driving signal which causes undesired circulating energy loss. Moreover, the sensed $v_{DS}$ of the MOSFET is actually the sum of the $R_{ds\_on}$ voltage drop and the package's inductive voltage drop. A nano Henry (nH) inductance introduced by PCB trace will cause a considerable duty cycle loss[4]. Therefore, the SR will be on for a much shorter time than required, resulting in extra conduction loss.

The conventional DCR (DC resistance of the inductor) current sensing method is widely used to sense and emulate the current of in VRs[9-11]. The advantages of this method are that it utilizes the parasitic DCRs of the inductors and is intrinsically lossless[12-14]. Literature [4] tries to use DCR current sensing method to compensate the duty cycle loss caused by the trace inductance of the MOSFET package. However, there are too many active switches used in the matching circuit that makes the compensator too complicated to implement. In addition, active switches also degrade the reliability of the power circuit. Moreover, the compensator has no filter function such that the false-triggering problem caused by the parasitic ringing can not be solved.

In this paper, a new driving method for the SR based on the $v_{DS}$ sensing scheme is presented. By applying a zero-

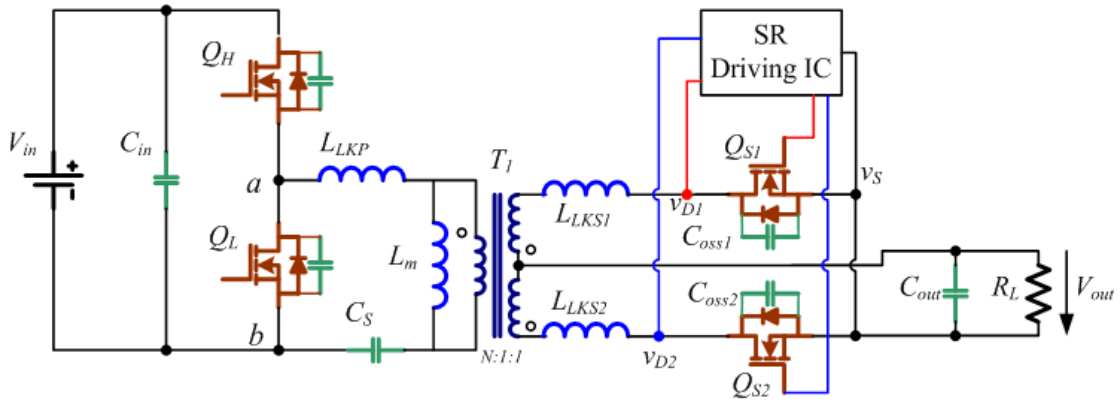


Fig. 1. Typical half-bridge LLC resonant converter with SRs

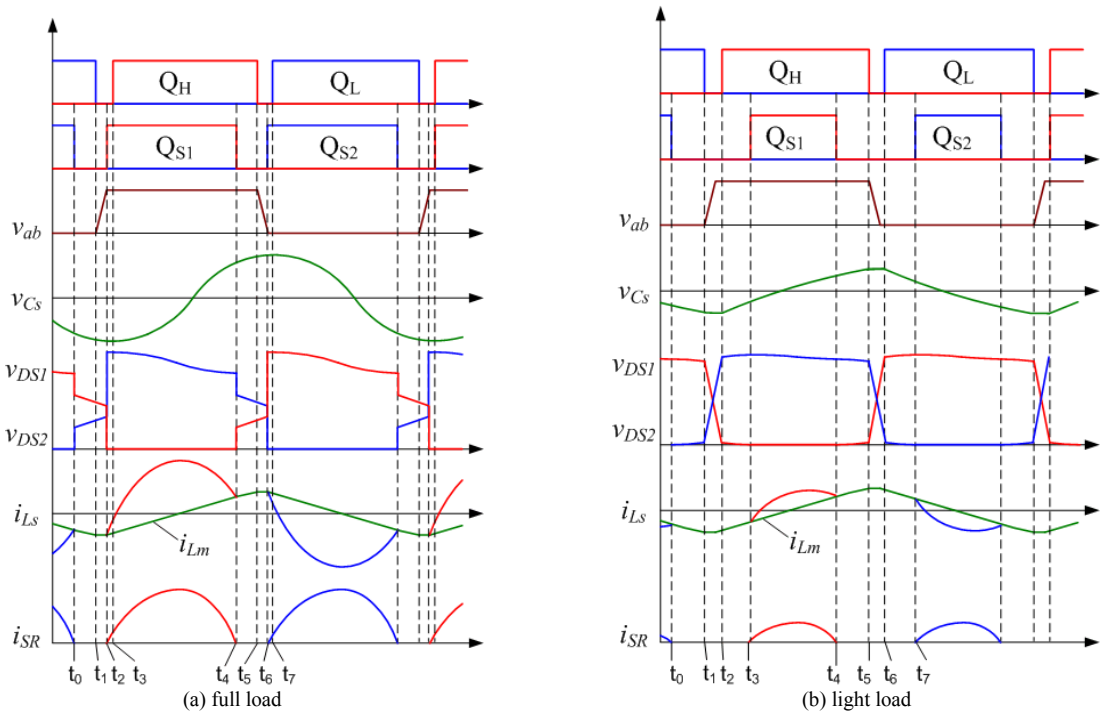


(a) full load (b) light load

Fig. 2. Key waveforms of the LLC converter operated in full load and light load condition

crossing noise filter between the drain to the source of the SR, the false triggering can be effectively eliminated. The resistor and the capacitor in the filter are also used to compensate the duty cycle loss caused by the trace inductance of the MOSFET package. There are only three passive components in this filter, making the driving scheme reliable and easy to implement. A 400V to 12V 600W half bridge LLC resonant converter prototype is built to validate the theoretical analysis.

## II. Problems of The Traditional Voltage Sensing SRs Driving Method

Fig. 1 shows the circuit diagram of the typical half-bridge LLC resonant converter with SRs. $L_{LKP}$ is the primary side leakage inductance of the transformer. $L_{LKS1}$ and $L_{LKS2}$ are the secondary leakage inductance. $C_{oss1}$ and $C_{oss2}$ are the output capacitance of the SRs. Fig. 2 shows the key waveforms of the LLC converter when operated in full load and light load conditions. It is observed that the primary side driving signals can not be applied to the SRs because of the nonlinear characteristics. To drive the SRs properly, the $v_{DS}$ of the SRs can be used. However, some problems should be solved before applying this method.

### A. *False-triggering at the turn on of SRs*

As shown in Fig. 2, there is a small interval when both of the two SR MOSFETs turn off ($t_4$~$t_6$ in Fig. 2 (a) and $t_4$~$t_7$ in Fig. 2 (b)). When the SRs turn off, $L_{LKP}$, $L_{LKS1}$ and $L_{LKS2}$ resonate with the output capacitance ($C_{oss}$) of the SRs. As

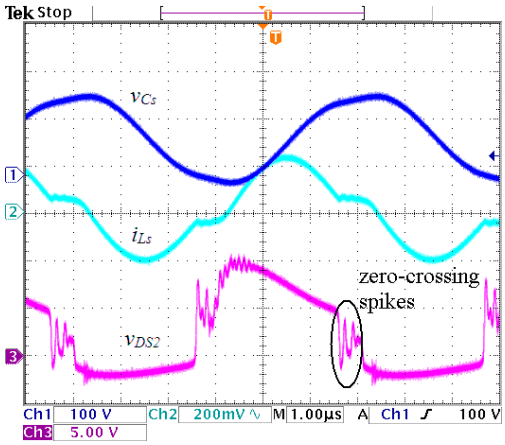


Fig. 3. Parasitic ringing of the $v_{DS}$ when the SRs turned off

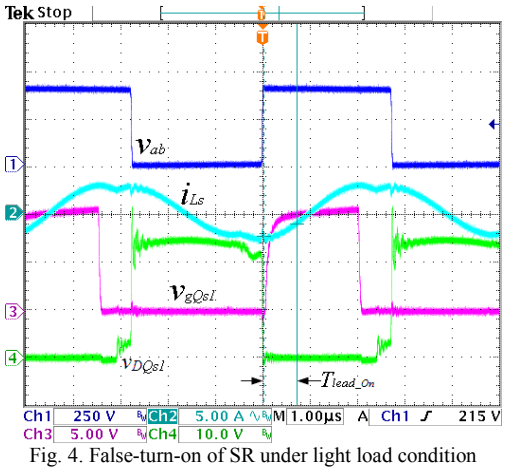


Fig. 4. False-turn-on of SR under light load condition

shown in Fig. 3, the voltage $v_{DS2}$ has many high frequency spikes when the $Q_{S1}$ turns off. If the voltage spikes reach the SRs turn on threshold, the SRs will be false-triggered. Fig. 4 shows the false-turn-on of the SR at light load condition. This will result in the energy reverse from the output capacitor to the input source, or even worse breakdown of the power circuit.

One possible solution to prevent the false-triggering at turn-on of the SRs is to add a RC filter to absorb the voltage spikes of the $v_{DS}$, as shown in Fig. 5. The $v_{filter}$ is used as a substitute for the $v_{DS}$, and sensed by the driving IC to generate the gate signal.

Due to the high frequency of the voltage spikes, the time constant of the RC filter should be very small. The equivalent circuit of the parasitic ringing is shown in Fig. 6. Comparing the leakage inductance of the transformer with the output capacitance of the SRs, the influences of the magnetizing inductance $L_m$, the series resonant capacitor $C_S$ and the output capacitor $C_{out}$ can be neglected. To simplify the analysis, suppose that

$$L_{LKS1} = L_{LKS2} = L_{LKS}$$
$$C_{oss1} = C_{oss2} = C_{oss} \quad (1)$$

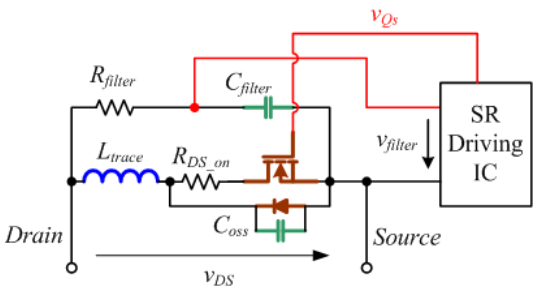


Fig. 5. $v_{DS}$ sensing method with a RC filter

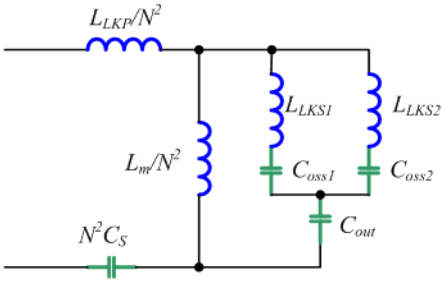


Fig. 6. Equivalent circuit of the parasitic ringing

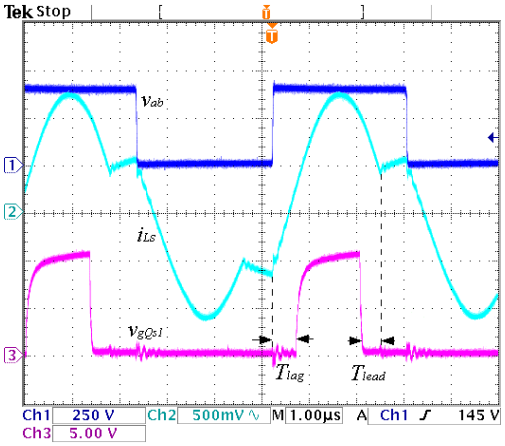


Fig. 7. Experiment result of the triggering signal of the SR with RC filter

The ringing frequency can be derived as

$$f_{ripple} = \frac{1}{2\pi \cdot \sqrt{\left(\frac{L_{LKP}}{N^2} + \frac{L_{LKS}}{2}\right) \cdot 2C_{oss}}} \quad (2)$$

The time constant of the RC filter should be selected a little larger than the period of the parasitic ringing. Fig. 7 shows the experiment results of the RC filter scheme. By applying a small time constant (about 100ns), the false-triggering phenomenon is effectively eliminated.

Unfortunately, it is observed that the driving signal of SR in Fig. 7 has an unacceptably large lag time at the switch on and a lead time at the switch off which will cause considerable conduction loss of the SR body diode. The reason for the delay at switch on is that the capacitor in the

RC filter sustains a high positive voltage before the body diode conducts, and then discharge slowly to the turn-on threshold (less than 0V). Fig. 8(a) shows the equivalent circuits of the SR with RC filter during the body diode conduction interval. When the body diode of the SR starts to conduct, as shown in Fig. 8(b), the detected $v_{filter1}$ is larger than the output voltage $V_{out}$ at $t_1$. During $t_1$~$t_2$, the body diode of the $Q_{S1}$ is forward biased and clamps the $v_{DS1}$ to the forward voltage of the body diode $-V_{Fb}$. Corresponding to the time constant of the RC filter, $v_{filter1}$ starts to decrease to the turn on threshold slowly.

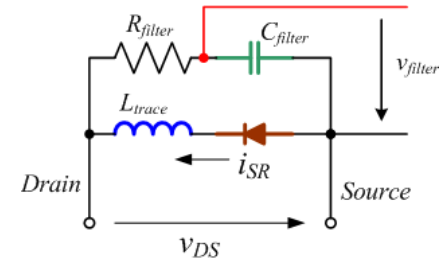


(a) equivalent circuit during body diode conduction

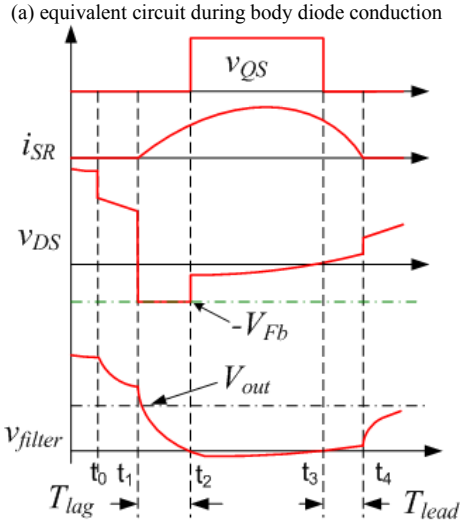


(b) key waveforms

Fig. 8. Operation of the SR with RC filter

## B. *Duty cycle loss at the turn off of SRs*

As to the lead time at the switch off, the impedance of the $C_{oss}$ is much larger than the $R_{DS\_on}$ and can be neglected, therefore, only the trace inductance of the SR package should be taken into account. As shown in Fig. 8(b), the current through the SR can be treated as part of a sinusoid waveform, and the frequency of the sinusoid waveform is equal to the series resonant frequency of the resonant tank. Because of the trace inductance, the voltage $v_{DS}$ leads the current $i_{SR}$. The lead angle and the lead time of the $v_{DS}$ to the $i_{SR}$ can be derived as

$$\theta_{lead} = \tan^{-1}\left(\frac{\omega_0 \cdot L_{lead}}{R_{DS\_on}}\right) \tag{3}$$

$$T_{lead} = \frac{\theta_{lead}}{\omega_0} \tag{4}$$

where $\omega_0$ is the series resonant frequency of the resonant tank. It is observed that if the $v_{DS}$ is detected directly to generate the driving signal of SR, the duty cycle loss is inevitable. Fig. 9 shows the lead-turn-off of the SR when $v_{DS}$ of the SR is fed to the driving IC.

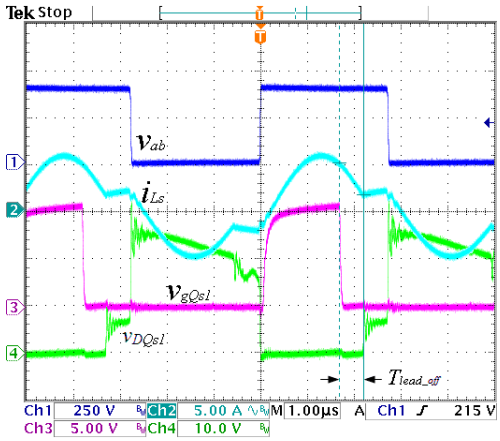


Fig. 9. Lead-turn-off of the SR

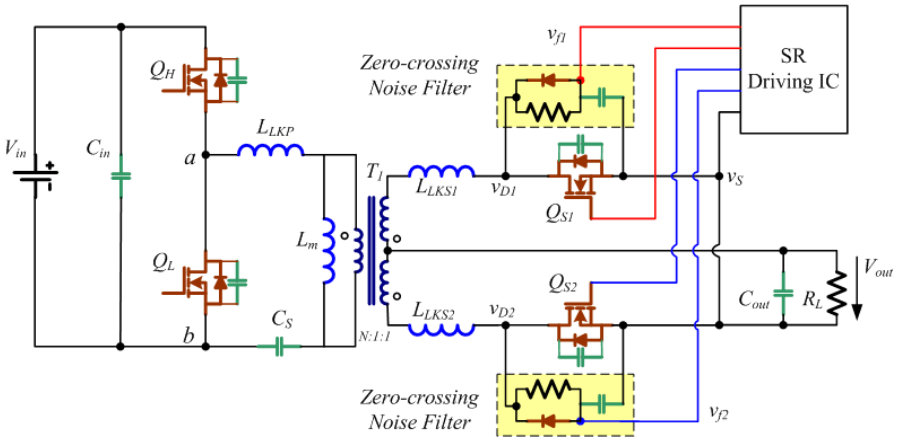


Fig. 10. Circuit diagram of the half-bridge LLC resonant converter with SRs and zero-crossing noise filter

## III. New Driving Method for SRs with Zero-crossing Filter

To solve the turn-on delay problem, an anti-parallel diode can be added to discharge the RC filter capacitor quickly. Fig. 10 shows the circuit diagram of the half-bridge LLC resonant converter with SRs and zero-crossing filter. In the diagram, $v_{f1}$ and $v_{f2}$ are sensed by the SR driving IC as the substitutes of $v_{D1}$ and $v_{D2}$. The equivalent circuit of the SR with zero-crossing noise filter is shown in Fig. 11 in which the forward voltage of the $D_{filter}$ ($V_{FD}$) should be a little larger than that of the body diode of the SR ($V_{Fb}$). Two diodes need to be connected in series if this condition can not be met by one diode.

To compensate the lead time at the switch off of the SR, traditional DCR current sensing method can be applied. The parameters of the zero-crossing noise filter should be selected carefully to match the trace inductance and $R_{DS\_on}$ of the SR. As shown in Fig. 12, the parameters of the filter are chosen specifically to emulate the lead angle $\theta_{lead}$ so that the voltage across the $C_{filter}$ can describe $v_{RDS\_on}$ exactly. The parameters of the filter is defined as

$$R_{filter}C_{filter} = \frac{L_{trace}}{R_{DS\_on}} \quad (5)$$

The equivalent circuit diagrams of the SR with the zero-crossing noise filter of each operation mode are shown in Fig. 14. The key waveforms of the SR with zero-crossing filter under different load conditions are illustrated in Fig. 13. It's assumed that $Q_H$ is OFF and $Q_L$ is ON before $t_0$.

1. Before $t_0$, all of the SRs are turned off. There is only the magnetizing current discharging the resonant capacitor. At $t_0$, the primary MOSFET $Q_L$ turns off The voltage across the SR decreases quickly, and reaches to the forward voltage drop $V_{Fb}$ of the SR body diode at $t_1$. At the same time, $C_{filter}$ is discharged through $D_{filter}$ until the voltage across $C_{filter}$ equals to $V_{FD}$- $V_{Fb}$ in which $V_{FD}$ is the forward voltage drop of $D_{filter}$.
2. At $t_1$, Due to the existence of $C_{oss}$ of the SR, the voltage $v_{DS}$ has some high frequency ringing which has been explained in previous section. The peak voltage of the

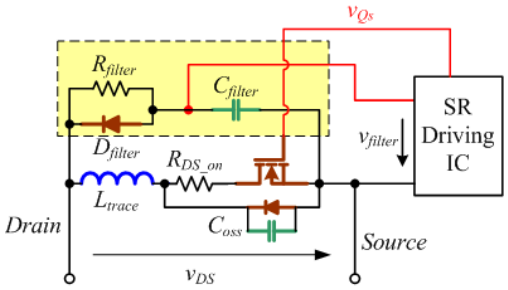


Fig. 11.Equivalent circuit of the SR with the zero-crossing noise filter

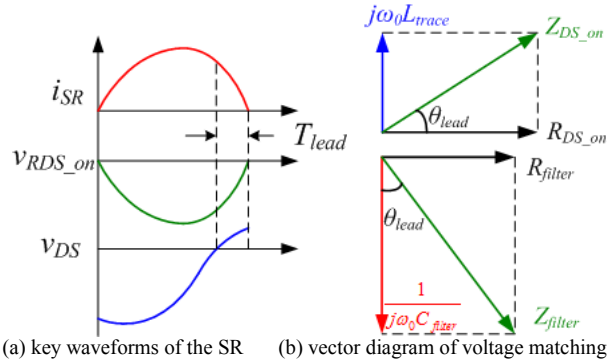


(a) key waveforms of the SR (b) vector diagram of voltage matching

Fig. 12.Voltage matching method for the SR with the zero-crossing noise filter

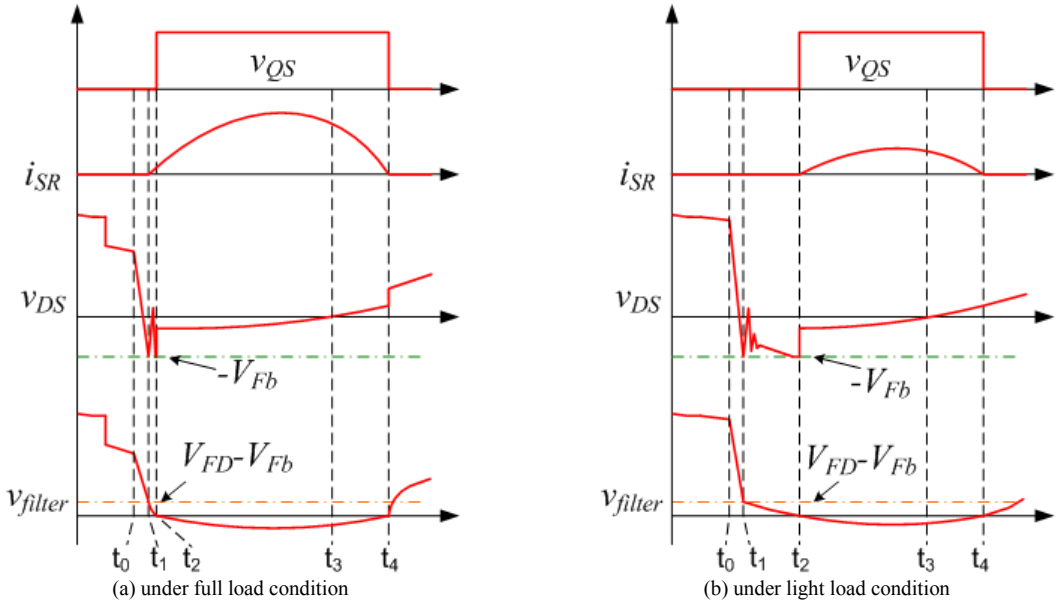


(a) under full load condition (b) under light load condition

Fig. 13. Key waveforms of the SR with the zero-crossing noise filter

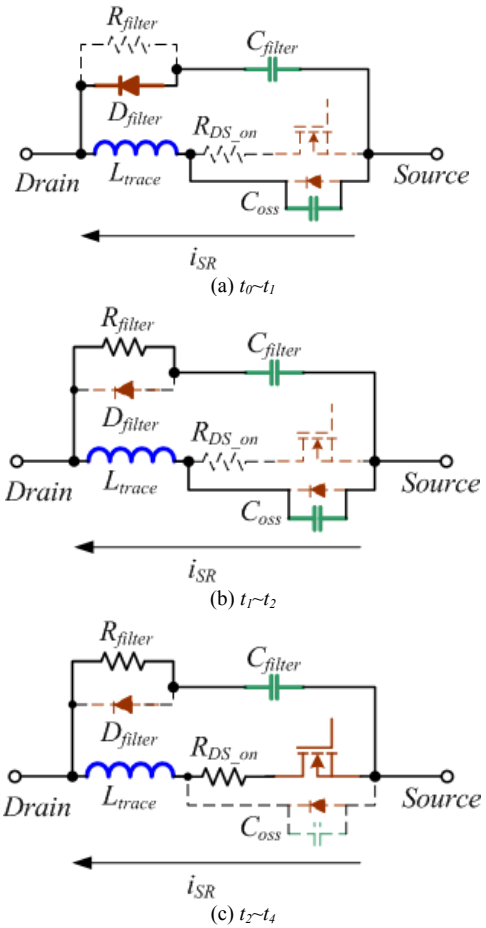


Fig. 14. Operation modes of the SR with the zero-crossing noise filter

ringing is limited by the forward voltage drop $V_{Fb}$ of the SR body diode. Meanwhile, $R_{filter}$ and $C_{filter}$ together work like a RC filter and filter out the high frequency ringing.

3. Before $t_2$, the body diode of the $Q_{S1}$ is forward biased and clamps $v_{DS}$ to $-V_{Fb}$. At $t_2$, the voltage across $C_{filter}$ $v_{filter}$ reaches to the turn on threshold of the driving chip so the driving signal is generated. During $t_2$~$t_4$, $R_{filter}$ and $C_{filter}$ together work like a traditional DCR current sensing circuit to emulate the current through the SR. At $t_4$, the voltage $v_{filter}$ reaches to the turn off threshold of the driving chip. The SR is turned off.

There are two premises for the zero-crossing filter to emulate the current through the SR. One is that the parameters of the $R_{filter}$ and $C_{filter}$ should be matched to the trace inductance and $R_{DS\_on}$ of the SR, as shown in equation (5). The other is that the initial condition of the voltage $v_{filter}$ is zero. Due to the deliberately designed parameters of the $R_{filter}$ and $C_{filter}$ as well as the small value between $V_{FD}$-$V_{Fb}$ and the turn on threshold, both of these two premises can be met. In addition, the false-triggering immunity of the zero-crossing noise filter is still retained. Consequently, the reliability of the circuit is improved and the conduction loss is significantly reduced.

## IV. Simulation and Experimental Results

To verify the theoretical analysis in the previous section, a prototype of 400V/12V 600W half bridge LLC resonant converter with SRs is built. The parameters of the circuit are listed in Tab. 1.

Tab. 1. Parameters of the Prototype

| | | | |
|---|---|---|---|
| $L_m$ (μH) | 98.7 | $C_S$ (nF) | 40 |
| $L_{LKP}$ (μH) | 6.8 | $R_{filter}$ (kΩ) | 3.9 |
| $L_{LKS}$ (nH) | 9 | $C_{filter}$ (pF) | 100 |
| $D_{filter}$ | 1N4148 | | |
| SR driving IC | IR1168 | $Q_H$, $Q_L$ | IPB50R299CP |
| Turns ratio | 20:1:1 | $Q_{S1}$, $Q_{S2}$ | SIR158DP |

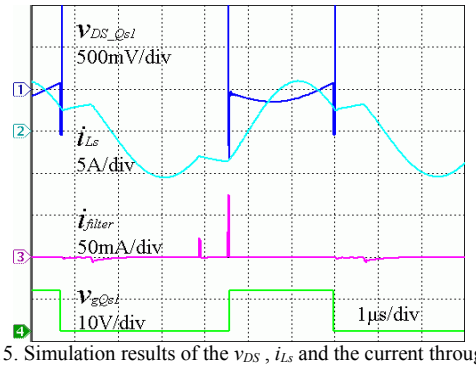


Fig. 15. Simulation results of the $v_{DS}$ , $i_{Ls}$ and the current through the zero-crossing noise filter

Fig. 15 shows the simulation results of the $v_{DS}$, the current of the resonant tank and the current through the zero-crossing

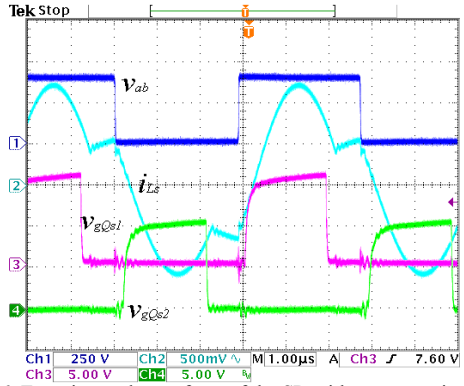


Fig. 16. Experimental waveform of the SR with zero-crossing noise filter at full load condition

noise filter. It is observed that the extra loss of the zero-crossing noise filter is tiny. A short delay at the switch on and a lead time at the switch off are left to prevent the energy reverse from the output capacitor to the source. Because of the small turn on and turn off currents of the SR, the conduction loss of the body diode can be neglected.

Fig. 16 and Fig. 17 illustrate the experimental waveforms of the SR with zero-crossing noise filter at full load and light load conditions. It shows that the SR with zero-crossing noise filter can operate properly at any load condition.

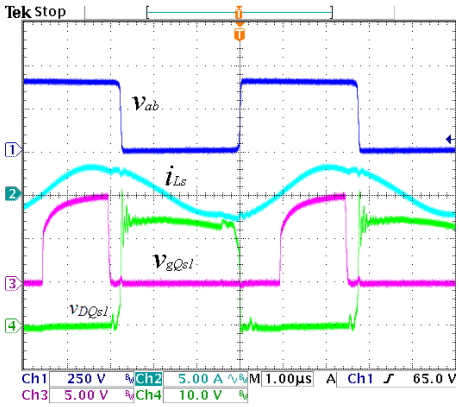


Fig. 17. Experimental waveform of the SR with zero-crossing noise filter at light load condition

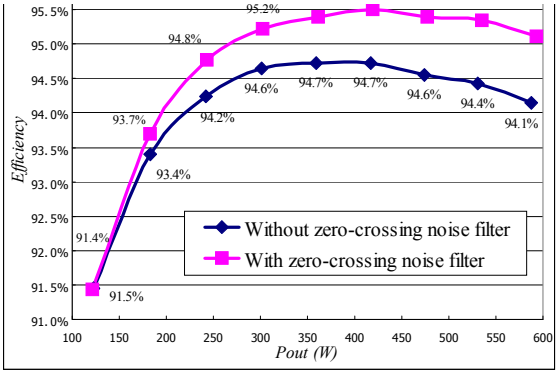


Fig. 18. Efficiency comparison of the circuit with and without the zero-crossing noise filter

Fig. 18 compared the measured efficiency between the prototype with and without zero-crossing noise filter at different load condition. When the load current increases, the efficiency improvement caused by the proposed filter becomes more significant.

## V. Conclusion

In this paper, a new driving method for SRs in LLC resonant converter is presented. By applying a zero-crossing noise filter to the SRs, the false-triggering problem at the turn-on of the SRs caused by the parasitic ringing is prevented and the reliability of the power circuit is greatly improved. Moreover, the parameters of the zero-crossing noise filter should be selected specifically to turn off SR exactly when its current falls to zero. Consequently, the body diode conduction loss is significantly diminished which makes sinking the heat by the footprint possible. This zero-crossing noise filter can also be applied to any other SR circuit operated in DCM mode. A 400V to 12V 600W half bridge LLC resonant converter prototype is built to verify the theoretical analysis.

## References


[1] A. Lokhandwala, M. Salato, and M. Soldano, "Dual SmartRectifier and DirectFET Chipset Overcomes Package Source Inductance Effects and Provides Accurate Sensing for Synchronous Rectification in DC-DC Resonant Converters," in *Proc. IEEE Appl. Power Electron. Conf.*, 2007, pp. 1559-1562.

[2] B. Lu, W. Liu, L. Yan, *et al.*, "Optimal design methodology for LLC resonant converter," in *Proc. IEEE Appl. Power Electron. Conf.*, 2006, pp. 533-538.

[3] B. Wang, X. Xin, S. Wu, *et al.*, "Analysis and Implementation of LLC Burst Mode for Light Load Efficiency Improvement," in *Proc. IEEE Appl. Power Electron. Conf.*, 2009, pp. 58-64.

[4] D. Fu, Y. Liu, F. C. Lee, *et al.*, "A Novel Driving Scheme for Synchronous Rectifiers in LLC Resonant Converters," *IEEE Trans. Power Electron.*, vol. 24, no. 5, pp. 1321-1329, 2009.

[5] G. Zhang, J. Zhang, C. Zhao, *et al.*, "LLC resonant DC/DC converter with current-driven synchronized voltage-doubler rectifier," in *Proc. IEEE Energy Conv. Cong. Expos.*, 2009, pp. 744-749.

[6] B. Yuan, M. Xu, X. Yang, *et al.*, "A new structure of LLC with primary current driven synchronous rectifier," in *Proc. IEEE Power Electron. Motion Control Conf.*, 2009, pp. 1266-1269.

[7] C. Zhao, B. Li, J. Cao, *et al.*, "A novel primary current detecting concept for synchronous rectified LLC resonant converter," in *Proc. IEEE Energy Conv. Cong. Expos.*, 2009, pp. 766-770.

[8] X. Xie, J. C. P. Liu, F. N. K. Poon, *et al.*, "A novel high frequency current-driven synchronous rectifier applicable to most switching topologies," *IEEE Trans. Power Electron.*, vol. 16, no. 5, pp. 635-648, 2001.

[9] R. Lenk, "Application Bulletin AB20 Optimum Current-Sensing Techniques in CPU Converters," *Fairchild Semiconductor Application Notes*, 1999.

[10] E. Dallago, M. Passoni, and G. Sassone, "Lossless current sensing in low-voltage high-current DC/DC modular supplies," *IEEE Trans. Ind. Electron.*, vol. 47, no. 6, pp. 1249-1252, 2000.

[11] H. P. Forghani-zadeh and G. A. Rincon-Mora, "Current-sensing techniques for DC-DC converters," in *Proc. Circuits and Systems, 2002. MWSCAS-2002. The 2002 45th Midwest Symposium on*, 2002, pp. II-577-II-580 vol.2.

[12] H. Lei and L. Shiguo, "Design considerations of time constant mismatch problem for inductor DCR current sensing method," in *Proc. IEEE Appl. Power Electron. Conf.*, 2006, p. 7 pp.

[13] D. Yan, X. Ming, and F. C. Lee, "DCR Current Sensing Method for Achieving Adaptive Voltage Positioning(AVP) in Voltage Regulators with Coupled Inductors," in *Proc. IEEE Power Electron. Soc. Conf.*, 2006, pp. 1-7.

[14] H. Lei and L. Shiguo, "Design Considerations for Small Signal Modeling of DC-DC Converters Using Inductor DCR Current Sensing Under Time Constants Mismatch Conditions," in *Proc. IEEE Power Electron. Soc. Conf.*, 2007, pp. 2182-2188.